



Conformational changes of photoactive yellow protein monitored by terahertz spectroscopy

E. Castro-Camus, M.B. Johnston *

Department of Physics, University of Oxford, Clarendon Laboratory, Parks Road, Oxford OX1 3PU, United Kingdom

ARTICLE INFO

Article history:

Received 22 August 2007

In final form 18 February 2008

Available online 2 March 2008

ABSTRACT

Observing the structural dynamics of proteins under conditions as close as possible to those in a living organism is essential for understanding the biological functions of proteins accurately. Here we demonstrate that terahertz spectroscopy is a convenient probe of conformational changes in proteins suspended in physiological buffer solution. We have observed that the partial unfolding of photoactive yellow protein leads to a clear increase in absorption at terahertz frequencies. Using normal mode and molecular dynamics simulations we show that this increase in absorption is related to an increase in the density of delocalised vibrational modes in the more flexible partially unfolded state.

© 2008 Elsevier B.V. All rights reserved.

1. Introduction

The photoactive yellow protein (PYP) from *Ectothiorhodospira halophila* has recently become a model system for the study of conformational changes in proteins [1], because it is relatively small (125 residues) and undergoes a reversible change in tertiary structure when illuminated with blue light [2]. The majority of studies on the relationship between the structure and function of proteins such as PYP have relied on X-ray diffraction data from crystallised proteins [3,4]. Observing conformational changes in the crystallised forms of a protein is a first approximation to the *in vivo* states. However, suspending proteins in physiological buffer solution is clearly a much better approximation to the *in vivo* environment. Unfortunately, experimental investigations of protein dynamics in solution have proved challenging. Time-resolved fluorescence spectroscopy [5] and two-dimensional infrared spectroscopy [6] are techniques that have provided valuable information about protein dynamics. Some of the most promising results have been obtained using nuclear magnetic resonance [2] (NMR), although even these studies have so far been restricted to a few proteins of suitable size.

Ultraviolet, visible and infrared spectroscopy are important tools in the field of structural biology. In particular UV circular dichroism [7] spectroscopy and Fourier transform infrared spectroscopy [8,9] are commonly used analytic methods. In contrast, relatively little is known about protein spectroscopy in the far-infrared region of the spectrum. Spectroscopy in the mid- and near-infrared ($\sim 20\text{--}300\text{ THz}$; $600\text{--}10\,000\text{ cm}^{-1}$) regions of the spectrum probe vibrations associated to localised atom–atom stretches, whereas far-infrared or terahertz radiation ($\sim 100\text{ GHz}\text{--}10\text{ THz}$;

$3\text{--}300\text{ cm}^{-1}$) probes delocalised collective vibrational modes in proteins [10].

Studying the terahertz-frequency collective modes of proteins is vital to understanding the relationship between their conformation and function [11–13]. There is also evidence that collective modes could be used to characterise proteins within families [14]. Protein motion can be thought of as a superposition of many normal modes of vibration. The terahertz-frequency modes will change with any structural reconfigurations of the protein. In this way the terahertz normal modes can be related to the structure and function of a protein. The normal mode vibrations interact with electromagnetic radiation since proteins are composed of polar and polarisable molecular units. Therefore, terahertz absorption spectroscopy can be used to probe the normal modes and hence for protein structure and function studies.

Terahertz time-domain spectroscopy (THz-TDS) [15–17] is a powerful technique developed over the last two decades covering the far-infrared or terahertz band of the spectrum. Performing terahertz spectroscopy on proteins in aqueous solution is challenging, owing to the poor transmission of water in this spectroscopic range [18], yet the potential of this technique has recently generated interest from both the biochemical and terahertz spectroscopy communities [19–22].

The ground state of photoactive yellow protein (pG) shown in Fig. 1 consists of a 6-stranded antiparallel β -sheet that is relatively stable and rigid, flanked by several α -helices that are more flexible [23]. Photoexcitation of PYP induces a series of changes leading to a conformational reconfiguration of the protein: The photocycle of PYP involves a *trans*–*cis* isomerisation of the chromophore *p*-coumaric acid [24], which is covalently linked to the polypeptide through Cys69 and surrounded by a hydrogen-bond network involving residues Cys69, Glu46, Tyr42 and Thr50. After photoexcitation the link between the chromophore and Glu46 is broken and

* Corresponding author.

E-mail address: m.johnston@physics.ox.ac.uk (M.B. Johnston).

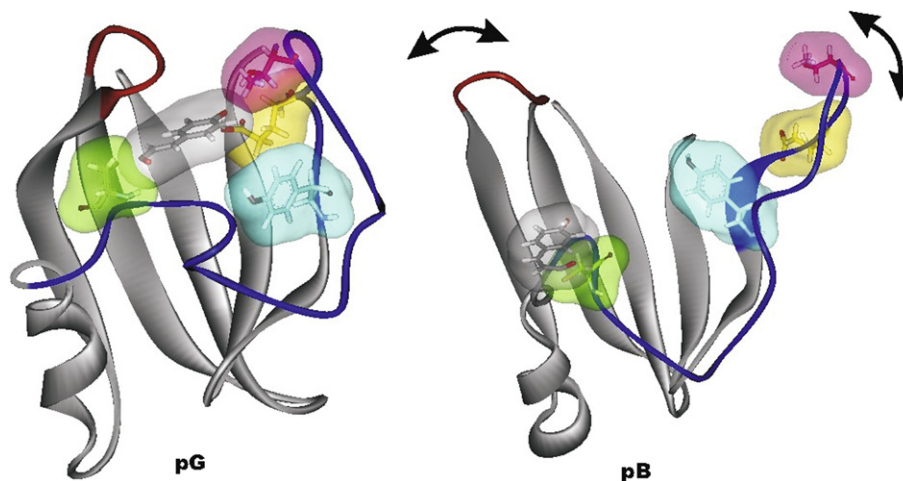


Fig. 1. Schematic representations of PYP. pG (PDB: 1XFN) and pB (PDB: 1XFQ) corresponding to the ground state and photo-intermediate structures of $\Delta 25$ -PYP measured by NMR [23] showing the partial unfolding of PYP. Colours point out the upper (red) and lower (blue) loops which are the segments of greatest change in flexibility from one conformation to the other. Residues 42, 46, 50 and 69 are shown in cyan, yellow, magenta and green respectively, and the chromophore *p*-coumaric acid is shown in grey.

over the following few milliseconds PYP undergoes a partial unfolding as shown in Fig. 1 (pB). This semi-unfolded structure is called photo-intermediate (pB).

Recently published NMR measurements [23] on a truncated mutant of PYP ($\Delta 25$ -PYP) revealed that there is an increase in flexibility in the semi-unfolded pB state compared with the fully folded pG state. This increased flexibility is particularly noticeable in the regions marked in Fig. 1. The NMR measurements estimate that the motion of residues 42–44, 47, 48–52, 62 and 66 (lower arm marked in the pB structure on Fig. 1) as well as residue 97 (higher arm marked in the pB structure on Fig. 1) occurs on a sub-nanosecond to picosecond time-scale. Such motion is associated with frequencies of hundreds of GHz to a few THz. In addition to the NMR measurements, molecular dynamics simulations [25] of pG and pB structures in PYP have predicted an increase in root-mean-square position fluctuations, supporting a qualitative picture of large sections of the protein having greater flexibility. The statistical mechanical modelling presented in Ref. [26] also predicts an increase in the correlation of motion of all residues, suggesting the formation of vibrational modes involving the entire structure. Here we report measurements of the terahertz frequency absorption change of PYP induced by a change of configuration. We discuss the physical origin of the absorption change based on molecular dynamics simulations and normal mode analysis.

2. Experiment

2.1. Protein extraction

Escherichia coli was used to express the A5C mutant of photoactive yellow protein and then the protein was extracted and purified by histidine-tag nickel-column purification, followed by gel filtration. The sample was concentrated by centrifugation up to ~ 1 mM and kept in Tris–HCl buffer (pH ~ 7.8). This particular mutant was chosen because it has a long-lived photo-intermediate state.

2.2. Terahertz spectroscopy

A very sensitive terahertz time-domain spectroscopy system [17] was used to measure the absorption in the frequency (wave-number) range from 100 GHz (3 cm^{-1}) to 2 THz (66 cm^{-1}). The PYP solution ($\sim 10\ \mu\text{l}$) was encapsulated in a liquid phase cell, be-

tween two z-cut quartz windows separated $25\ \mu\text{m}$ using a Teflon spacer. Single-cycle pulses of THz radiation were produced by exciting a 3-mm thick semi-insulating GaAs photo-conductive switch with near-infrared pulses from a mode-locked Ti:sapphire laser (800 nm centre wavelength, 10fs pulse duration, 75 MHz repetition rate, and 320 mW average power) [17]. The THz pulses were focused onto the sample of PYP solution using off-axis parabolic mirrors. The THz radiation was detected using the technique of electro-optic sampling, using a $200\text{-}\mu\text{m}$ thick (110) ZnTe crystal mounted on 6-mm (100) ZnTe substrate.

Four blue (450 nm) high intensity light emitting diodes were used to illuminate the liquid sample uniformly ($\sim 35\text{ mW/cm}^2$) in order to trigger the pG to pB conformational change while terahertz radiation was used to probe the vibrational spectra of PYP. The THz path was enclosed in a dry nitrogen atmosphere in order to avoid atmospheric water vapour absorption. One hundred time-domain scans were taken for the dark and illuminated sample, in order to prevent long term drifts scans with and without light were recorded alternately, leaving 30 s between measurements to allow the protein to reach an equilibrium state.

The difference in absorption ($\Delta\alpha = \alpha_{\text{light}} - \alpha_{\text{dark}}$) as function of frequency, shown in Fig. 2, was calculated from the time-domain data as described in Ref. [27]. Error bars in Fig. 2a represent the first standard deviation of differential absorption over 100 measurements. The spectra were found to be reproducible across different preparations of PYP. A set of control experiments were also performed using just the buffer solution and confirmed that the signal did indeed come from photo-induced changes in PYP. We also discount the possibility of sample heating inducing a differential absorption signal, as the power density dissipated in the sample was small ($< 5\text{ mW/cm}^2$) and the sample was in good thermal contact with the environment via large quartz plates.

As can be seen in the figure the absorption of illuminated PYP (pB form) is greater than the absorption of the dark (pG) form for all frequencies between 0.25 and 2 THz. The absence of defined features is a consequence of the high density and broadness of collective vibrational modes, which is consistent with normal mode analysis of other proteins over this frequency range [12,28,29]. Earlier terahertz studies of proteins such as lysozyme have been restricted to measurements of the absorption of proteins in one structural form [13]. The measurements shown in Fig. 2 constitute the first observation of a change in THz absorption associated with a *functional reconfiguration* of a protein.

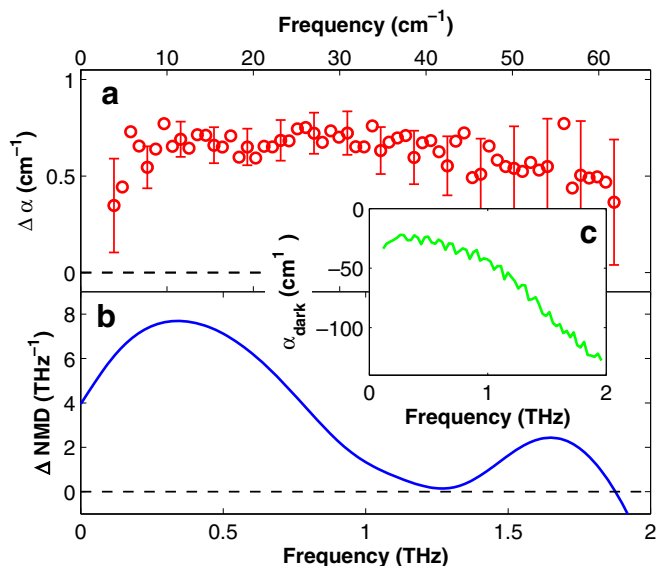


Fig. 2. The PYP solution shows an increase of absorption $\Delta\alpha = \alpha_{\text{light}} - \alpha_{\text{dark}}$ in the range from 0.25 to 2 THz between the pG and pB states (a). The error bars represent the standard error. (b) Difference in normal mode density $\Delta\text{NMD} = \text{NMD}_{\text{pB}} - \text{NMD}_{\text{pG}}$ between the light (pB) and dark (pG) states of PYP calculated by normal mode analysis. An increase of the low frequency normal mode density (NMD) of PYP in the pB state is seen. The augmentation of absorption is attributed to the increase of low frequency vibrational modes associated to large segments of the protein being able to vibrate freely in the semi-unfolded pB state. The inset shows the absorption spectrum of the PYP solution (dark state). Note that the absorption coefficient is negative, since it was calculated relative to the polar buffer solution [18].

3. Theoretical modelling and discussion

Molecular dynamics simulations and normal mode analysis are powerful tools that help us to understand conformational dynamics of proteins [28]. Molecular modelling toolkit [30] was used to calculate the first 4500 normal modes of $\Delta 25$ -photoactive yellow protein. Approximately 200 of those modes lie in the 0–2 THz range. Structures used for the calculation pG (1XFN) and pB (1XFQ) were obtained from www.pdb.org [23]. The Amber 94 force field was used; The structures were minimised and subsequently the normal modes were calculated. The first 6 normal modes associated to the translation and rotation of the protein were discarded and the remaining modes were used to calculate the normal mode density by convolving with a Gaussian of standard deviation $\sigma = 100$ GHz as follows $\text{NMD}(\nu) = \sum_{i=1}^N e^{-(\nu_i - \nu)^2 / \sigma^2} / \sigma \sqrt{2\pi}$.

The difference between the mode density of pB and pG is shown in Fig. 2b. From the plot it can be seen that the change of density of modes between the two conformations is positive for the full range between 0 and 2 THz. This demonstrates that the partially unfolded photo-intermediate structure has a higher density of vibrational modes within this low frequency region, which correspond to an enhancement of delocalised vibrations. A comparison of the two data sets in Fig. 2 reveals that there is a good correlation between the increase in absorption measured by terahertz spectroscopy and the calculated increase in normal mode density of the (illuminated) pB state compared with the (dark) pG state. The proportionality between the absorption and normal mode density is related to the distribution of charge across the whole protein, which leads to some collective modes being more dipolar in nature (and hence more able to interact with radiation) than others. Therefore each of the more than 200 modes present in the 0–2 THz range has a specific absorption cross-section. Hence the NMD calculations, which do not include these cross-sections, provide an indication of the absorption spectrum but not an exact fit to the data.

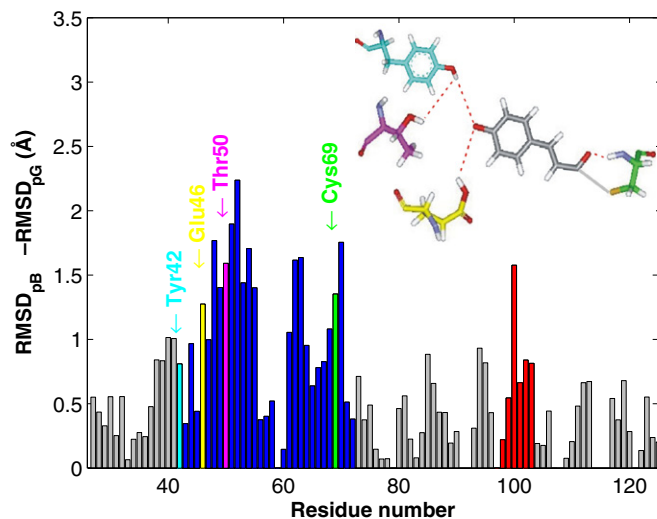


Fig. 3. Change in root-mean-square displacement (RMSD) between pB and pG conformations of $\Delta 25$ -PYP (PDB: 1XFN and 1XFQ [23]) calculated by molecular dynamics simulation for each residue. In blue are shown the residues from 42 to 72 that form the *lower loop*, and in red residues from 97 to 103 that form the *higher loop*. It is clear that these two regions are highly affected by the partial photo-induced unfolding. Residues 42, 46, 50 and 69 are shown in cyan, yellow, magenta and green. These residues together with the chromophore (grey) are central in the photocycle as they form a hydrogen-bond network (shown schematically on the top right corner). With the *trans-cis* isomerisation of the chromophore this network breaks, resulting in the partial unfolding of the structure and an increased flexibility of the protein.

In order to gain an in-depth understanding of the nature of these modes, the code NAMD [31] for scalable molecular dynamics modelling was used to perform a molecular dynamics calculation on the $\Delta 25$ -PYP structures pG (1XFN) and pB (1XFQ). The CHARMM all-hydrogen topology was used to generate the force field for the structures. A sphere of water was simulated to solvate the structures. NAMD was then used to equilibrate the structures at a temperature of 300 K using 250 000 time steps of 2 fs duration. Both structures reached equilibrium after ~ 70 and 350 ps reaching an average root-mean-square displacement (RMSD) per residue of ~ 1.7 and 3.2 Å, respectively. The RMSD for each residue was calculated from a further 50 000 steps (100 ps). The root-mean-square displacement difference between pB and pG is plotted for each residue in Fig. 3, where it can be seen that the mobility of almost all residues increases as the protein unfolds. However, the greatest increase is presented by the residues from 42 to 72 which form the *lower loop* marked blue in Fig. 3 (and schematically in Fig. 1) and from 97 to 103 that form the *higher loop* marked red in the figures. The lower loop is central in understanding the structural reconfiguration of PYP as it contains residues Tyr42, Glu46, Thr50 and Cys69 [1]. These residues form a hydrogen-bond network (shown in Fig. 3) that becomes unstable after the chromophore's isomerisation, and which is broken within a few milliseconds [8]. These hydrogen bonds link various points of the lower loop, restraining its motion. When the hydrogen-bond network is broken the lower loop becomes free to move and unfolds, producing a reconfiguration of the entire structure. The photo-intermediate structure has large segments with increased freedom of motion as demonstrated by the molecular dynamics simulation. Further analysis of the normal mode calculations in combination with the molecular dynamics simulation shows that the motion associated to the first few vibrational modes in pB has a strong RMSD contribution from residues in the lower and upper loops compared with the pG structure.

4. Conclusion

An increase in the absorption of the pB configuration in comparison to the pG state in the 0.25–2 THz range was observed experimentally. Normal mode calculations of both structures were performed, showing an increase in the density of normal modes in this spectral region for the photo-intermediate conformation in comparison with the ground state. A molecular dynamics simulation was used to identify changes in the average displacement of residues. Although almost all residues showed increased mobility, two particular regions (from residue 42 to 72 and from 97 to 103) of the protein showed the greatest increase. Thus we conclude that the experimentally observed absorption change is consistent with the photo-intermediate structure being more flexible and hence giving rise to a greater density of delocalised low frequency vibrational modes. Terahertz spectroscopy promises to be an invaluable tool in understanding the dynamics of proteins and monitoring conformational changes, by probing delocalised vibrational modes that depend on the overall structure.

Acknowledgements

The authors would like to thank J. van Thor for providing the PYP sample from the Biochemistry Department at the University of Oxford. They are grateful to P. Ramachandran who designed and created the A5C-PYP mutant used in this study. Finally, they would like to acknowledge financial support from the EPSRC (UK) and the Royal Society.

References

- [1] K.J. Hellingwerf, J. Hendriks, T. Gensch, *J. Phys. Chem. A* 107 (2003) 1082.

- [2] G. Rubinstenn, G.W. Vuister, F.A.A. Mulder, P.E. Dux, R. Boelens, K.J. Hellingwerf, R. Kaptein, *Nat. Struct. Biol.* 5 (1998) 568.
 [3] E.D. Getzoff, K.N. Gutwin, U.K. Genick, *Nat. Struct. Biol.* 10 (2003) 663.
 [4] U.K. Genick, S.M. Soltis, P. Kuhn, I.L. Canestrelli, E.D. Getzoff, *Nature* 392 (1998) 206.
 [5] B. Schuler, *ChemPhysChem* 6 (2005) 1206.
 [6] H.S. Chung, M. Khalil, A. Tokmakoff, *J. Phys. Chem. B* 108 (2004) 15332.
 [7] J. Sasaki, M. Kumauchi, N. Hamada, T. Oka, F. Tokunaga, *Biochemistry* 41 (2002) 1915.
 [8] L.J.G.W. van Wilderen, K.J. Hellingwerf, M.L. Groot, *Proc. Natl. Acad. Sci. USA* 103 (2006) 15050.
 [9] A.H. Xie, L. Kelemen, J. Hendriks, B.J. White, K.J. Hellingwerf, W.D. Hoff, *Biochemistry* 40 (2001) 1510.
 [10] J. Xu, K.W. Plaxco, S.J. Allen, *Protein Sci.* 15 (2006) 1175.
 [11] B. Brooks, M. Karplus, *Proc. Natl. Acad. Sci. USA* 80 (1983) 6571.
 [12] B. Brooks, M. Karplus, *Proc. Natl. Acad. Sci. USA* 82 (1985) 4995.
 [13] J. Xu, K.W. Plaxco, S.J. Allen, *J. Phys. Chem. B* 110 (2006) 24255.
 [14] S. Maguid, S. Fernandez-alberti, L. Ferrelli, J. Echave, *Biophys. J.* 89 (2005) 3.
 [15] M. Tonouchi, *Nat. Photon.* 1 (2007) 97.
 [16] C.A. Schmuttenmaer, *Chem. Rev.* 104 (4) (2004) 1759.
 [17] M. Johnston, L. Herz, A. Khan, A. Köhler, A. Davies, E. Linfield, *Chem. Phys. Lett.* 377 (1–2) (2003) 256.
 [18] J. Xu, K.W. Plaxco, S.J. Allen, *J. Chem. Phys.* 124 (2006) 036101.
 [19] J. Xu, K.W. Plaxco, S.J. Allen, *J. Phys. Chem. B* 110 (2006) 24255.
 [20] S.E. Whitmire, D. Wolpert, A.G. Markelz, J.R. Hillebrecht, J. Galan, R.R. Birge, *Biophys. J.* 85 (2003) 1296.
 [21] J.Y. Chen, J.R. Knab, J. Cerne, A.G. Markelz, *Phys. Rev. E* 72 (2005) 040901.
 [22] U. Heugen, G. Schwaab, E. Brundermann, M. Heyden, X. Yu, D.M. Leitner, M. Havenith, *Proc. Natl. Acad. Sci. USA* 103 (2006) 12301.
 [23] C. Bernard, K. Houben, N.M. Derix, D. Marks, K.J. Hellingwerf, R. Boelens, R. Kaptein, *Structure* 13 (2005) 953.
 [24] K. Heyne, O.F. Mohammed, A. Usman, J. Dreyer, E.T.J. Nibbering, M.A. Cusanovich, *J. Am. Chem. Soc.* 127 (2005) 18100.
 [25] I. Antes, W. Thiel, *Eur. Biophys. J.* 31 (2002) 504.
 [26] K. Itoh, M. Sasai, *Proc. Natl. Acad. Sci. USA* 101 (2004) 14736.
 [27] M. Yamaguchi, F. Miyamaru, K. Yamamoto, M. Tani, M. Hangyo, *Appl. Phys. Lett.* 86 (5) (2005) 053903.
 [28] H.W.T. van Vlijmen, M. Karplus, *J. Phys. Chem. B* 103 (1999) 3009.
 [29] A. Markelz, S. Whitmire, J. Hillebrecht, R. Birge, *Phys. Med. Biol.* 47 (2002) 3797.
 [30] K. Hinsien, *J. Comput. Chem.* 21 (2000) 79.
 [31] J.C. Phillips et al., *J. Comput. Chem.* 26 (2005) 1781.